JOURNAL OF MATERIALS SCIENCE 18 (1983) 2255–2259

Characterization of the current-blackening phenomena in scandia stabilized zirconia using transmission electron microscopy

F. K. MOGHADAM*, T. YAMASHITA, D. A. STEVENSON
Department of Materials Science and Engineering, Stanford University, Stanford, California 94305, USA

The nature of blackening of 8 mol % Sc_2O_3–ZrO_2, caused by imposing high current densities on this material at 800° C and $P_{O_2} < 10^{-7}$ atm, has been investigated by transmission electron microscopy. The material studied was in the form of hot pressed polycrystalline discs with equiaxed grains 2 to 4 μm in size with a cubic fluorite structure. There is also evidence of small coherent precipitates of tetragonal phase embedded within the matrix of the cubic fluorite phase. The current-blackened samples contained numerous polycrystalline aggregates, with crystallites 10 to 20 nm in size, and they were usually found at the grain boundaries. The lattice parameter of this phase is virtually identical to that of the original cubic-fluorite matrix phase. The electron diffraction pattern showed, however, weak reflections forbidden by the fcc symmetry of the parent phase. These reflections can only be indexed as primitive cubic, and it is proposed that grain boundary phase consists partly of non-stoichiometric zirconium suboxides (ZrO_{2-x}). The analysis of energy dispersive X-ray spectrum and electron diffraction patterns of the polycrystalline phase shows no evidence of the presence of metallic zirconium, as has been postulated previously.

1. Introduction

A phenomenon of considerable practical interest in the use of zirconia as a solid electrolyte is the discolouration (current-blackening) that results from the application of high current densities ($\gtrsim 5\,A\,cm^{-2}$) in reducing atmospheres. This discolouration is accompanied by an increase in the total conductivity, due to enhanced conduction [1], and also by a decrease in the fracture strength; extreme current-blackening will cause samples to crumble. Because of the obvious importance of these changes in the use of these electrolytes in oxygen sensors and for other applications, several studies of this phenomenon have been made [1–7]. These studies have determined the conditions leading to blackening and also have described the macroscopic changes that occur. Little information, however, has been presented concerning the microstructural changes and, in particular, the species responsible for the darkened colouration.

Oxides of di- or trivalent metals, such as Y^{3+}, Sc^{3+} or Ca^{2+} are added to zirconia both to stabilize or partially stabilize the high-temperature cubic phase and also to enhance the oxide vacancy concentration. The electrical conductivity in these materials is almost exclusively by the motion of oxide ion vacancies. When a current of about $5\,A\,cm^{-2}$ is applied to these electrolytes, blackening originates at the cathode and progresses towards the anode with a tongue shaped progression of the black region [3]. For a given current density and oxygen partial pressure, the position of the blackened zone depends on time. An interesting feature of the blackening process is its reversibility; a blackened sample reverts to its original state upon annealing in air or oxygen.

There are three possible mechanisms that have

*Present address: Intel Corporation, 2880 Northwestern Parkway MS SC3-307, Santa Clara, CA 95051, USA.

0022–2461/83 $03.00 + .12

been proposed for the current-blackening process:

1. The formation of F-centres
2. The formation of colloidal zirconium particles
3. The formation of a zirconium suboxide (ZrO_{2-x}).

Yanagida *et al.* [5] observed discolouration of a zirconia surface around a Pt-paste electrode at voltages greater than 2 V, and attributed this to F-centre migration away from the electrode region into the zirconia. An electron spin resonance (ESR) study by Thorp *et al.* [4] shows some evidence for the existence of F-centres but their result is contradicted by optical absorption studies [2, 3]. The blackened material exhibits complete absorption over the entire visible spectrum, from 300 to 700 nm, and shows no peaks which can correspond to F-centres.

Casselton [8] has proposed that F-centres are formed in the initial stages of blackening by electron injection into the crystal from the cathode by thermionic emission which then become trapped at anion vacancies forming the F-centres. Based on optical absorption studies, Wright *et al.* [3] suggests that these centres (F-centres) later coalesce and eventually lead to the deposition of colloidal particles of metallic zirconium in the 10 to 50 nm diameter range; however, this proposal has not been confirmed by direct observation of metallic precipitates. Both Pizzini *et al.* [9] and Gur [10] have shown the presence of fine particles (about 10 nm diameter) at the grain boundaries using SEM (scanning electron microscopy) with current-blackened zirconia; however, in neither case were the particles clearly identified. It is interesting that in alkali-halides, the formation of either F-centres or colloidal particles strengthens the material, presumably by a dislocation pinning mechanism [11–13]. In zirconia electrolytes, however, the situation is different; the mechanical properties deteriorate upon blackening. Guillou *et al.* [6] using a Pt-wire electrode observed blackening at 1250° C around the electrode under severe polarization (at voltages > 1 V) for $P_{O_2} < 10^{-6}$ atm, and attributed the blackening to the reduction of Zr^{4+} to Zr^{3+} (i.e. suboxide formation).

In the present study, a fully stabilized scandia-doped zirconia was current-blackened, and its microstructure was examined by transmission electron microscopy (TEM) in order to better understand the nature of the current-blackening mechanism.

2. Experimental methods

The samples used in this study were ZrO_2 + 8 mol % Sc_2O_3 electrolyte* in the form of discs 2.5 cm in diameter and 1 mm thick. The discs were hot pressed polycrystalline samples. Electron microprobe analysis (EDS) and EDS in conjunction with the TEM provided qualitative analysis of the samples, with the major impurities found to be iron, silicon and aluminium. More detailed microprobe analysis on ten different discs, using standards, established the levels to be about 2.0 wt % Fe, about 0.3 wt % Si, and about 0.06 wt % Al, with traces of nickel, potassium, chlorine, magnesium and phosphorus at levels of about 0.01 to 0.04 wt %. Porous gold electrodes were prepared by applying and firing gold paste† at 850° C. The cell temperature was maintained at 800° C under a reducing atmosphere ($P_{O_2} < 10^{-7}$ atm) on both the cathode and anode side of the cell. Blackening was induced by applying 2 V between the cathode and the anode. The voltage polarity was changed in order to induce blackening on both sides of the electrode, and this was repeated several times until the material became blackened throughout. The samples were then cooled rapidly in air.

Analysis of the samples were made by X-ray diffraction, optical microscopy and transmission electron microscopy. The TEM specimens were prepared from both the as-received (AR) and current-blackened samples from the above disc samples. The 3 mm diameter TEM discs were cut from several regions of the bulk, and mechanically thinned to 80 μm thickness. The final thinning was done by argon ion-beam milling to electron transparency (thickness = ~ 50 to 100 nm). A Philips EM400 transmission electron microscope equipped with a LaB_6 filament and energy dispersive X-ray spectrometer (EDS) was used throughout.

3. Experimental results

Optical microscopy on the current-blackened sample at magnifications up to 1000 x revealed no significant difference with the as-received sample, aside from the differences in colour. X-ray measurements on AR samples showed a cubic-fluorite

*Applied Electrochemistry Corporation, Sunnyvale, California.
†Engelhard Industries (No. A1560).

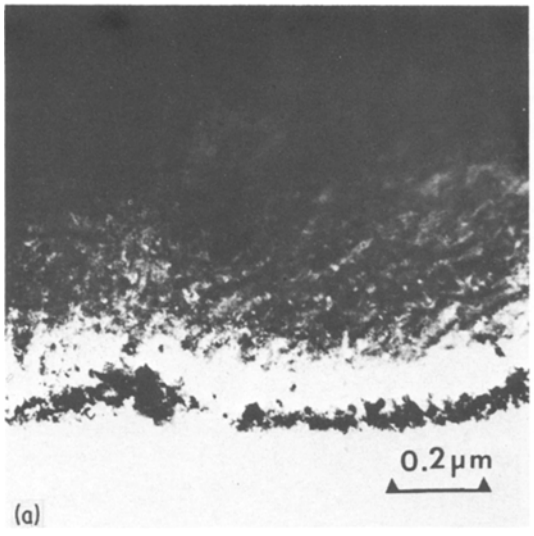

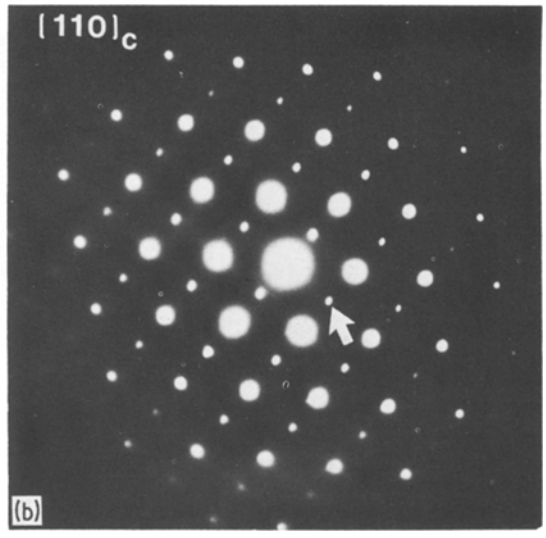

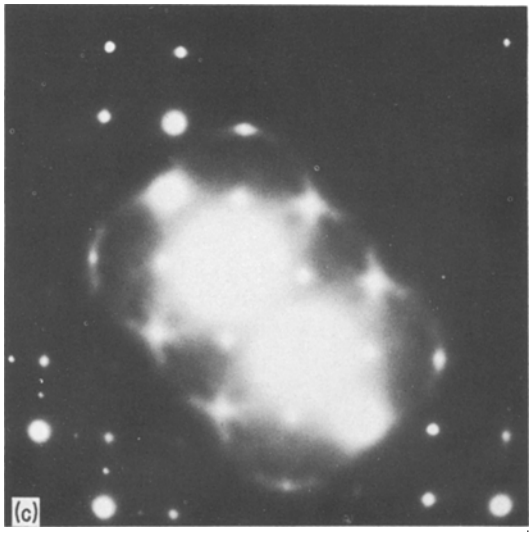

Figure 1 (a) A bright-field image of typical microstructure found in SSZ. (b) [110] cubic electron diffraction pattern from one of the grains shown in Fig. 1a. Fluorite-forbidden reflections are observed (arrowed). (c) Diffuse scattering observed in the electron diffraction pattern of a typical grain tilted away from [100] zone axis.

structure phase, with a lattice parameter of 0.51 ± 0.003 nm. Measurements on current-blackened samples showed no change in the structure nor the lattice parameter, a finding corroborated by previous studies [2, 3].

Several specimens from the AR sample were prepared and examined in the TEM to characterize the microstructure prior to current-blackening treatment. A bright-field (BF) image of typical microstructure is shown in Fig. 1a. Most of the grains were equiaxed, and typically 2 to 4 μm in diameter. A [110] electron diffraction pattern from one of the grains (Fig. 1b) is clearly that of cubic-fluorite structure, but fluorite-forbidden reflections are also observed (arrowed). This is probably due to the presence of small coherent precipitates of the tetragonal phase (α_2'). The phase diagram for the Sc_2O_3–ZrO_2 system [14, 15] for 8 mol% Sc_2O_3 shows cubic-fluorite solid solution as the stable phase at 800° C. At 500° C, a transformation from cubic to tetragonal is expected. The tetragonal (α_2') phase has a distorted fluorite structure, and it is detected by X-rays only in slowly cooled samples [15]. In the off-zone axis orientations, the electron diffraction pattern shows diffuse scattering, and both BF and DF (dark-field) images (Fig. 1c) show "mottled" contrast. These are characteristics of the presence of fine-scale particles in the initial stages of precipitation. It should be noted that yttria-stabilized zirconia exhibits similar contrast features in some of the grains, while most of the grains contain larger coherent tetragonal phase particles giving them a characteristic "tweed" pattern in the DF image [16]. The tetragonal particles are difficult to identify in the ZrO_2 system because the lattice parameters are usually very close to those of the cubic phase. In the present study a grain was occasionally observed to contain the rhombohedral β-phase ($Sc_2Zr_7O_{17}$). This was quite surprising since this phase only exists in the 11 to 13% Sc_2O_3 composition range from room temperature to 620° C [14]. For the development of this phase the sample must have an appreciable compositional inhomogeneity. This was confirmed from energy

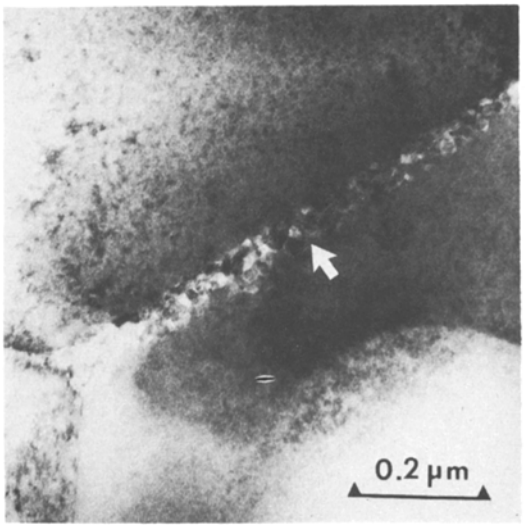

Figure 2 A bright-field image of small particles which had formed along the grain boundary (arrowed).

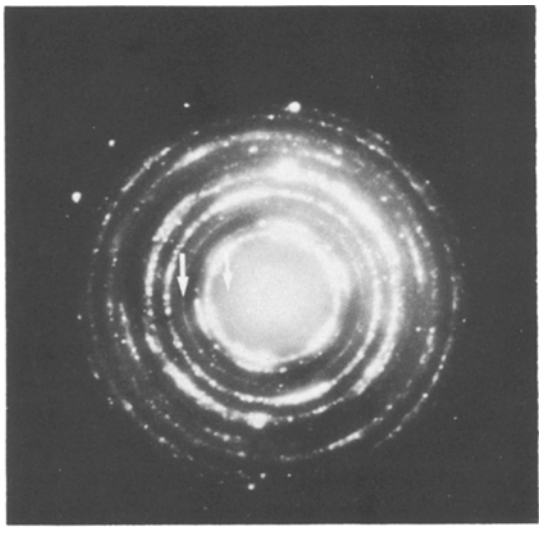

Figure 4 Electron diffraction pattern from the polycrystalline aggregate. Simple cubic reflections are arrowed.

dispersive X-ray spectra taken from several localized areas of the specimen. On the average, however, the scandium to zirconium ratio was close to the expected value of 5.5 to 1.0.

Several current-blackened specimens were examined in the TEM. Some specimens were more heavily blackened than the others. Typical microstructures that one observed in the lightly-blackened specimen are shown in Figs. 2 and 3. Many polycrystalline aggregates consisting of small particles approximately 10 nm in diameter were found, usually at the grain boundaries. These polycrystalline aggregates were uniformly distributed throughout the specimen. The diffraction pattern (Fig. 4) obtained from the polycrystalline aggregates shows that the particles are crystalline and there is no indication of "amorphous" character in the diffraction pattern. The particles appear to possess the same cubic-fluorite structure as the matrix grains. An interesting feature in the diffraction rings (Fig. 4) is that there are reflections which can only be indexed as the primitive-cubic equivalent of the cubic-fluorite structure, the implication being that there is a loss of symmetry which reduced the fcc cell to that of a primitive cubic cell. An energy dispersive spectrum (EDS) of the polycrystalline phase was taken using a small electron probe, and the measured zirconium to scandium ratio was identical to those of the nearby matrix grains within the limits of the analysis. The EDS analysis is not capable of distinguishing ZrO_2 from a suboxide. However, electron diffraction pattern analysis can distinguish pure zirconium from ZrO_2. Thus it appears that the aggregates do not contain any pure metallic zirconium phase.

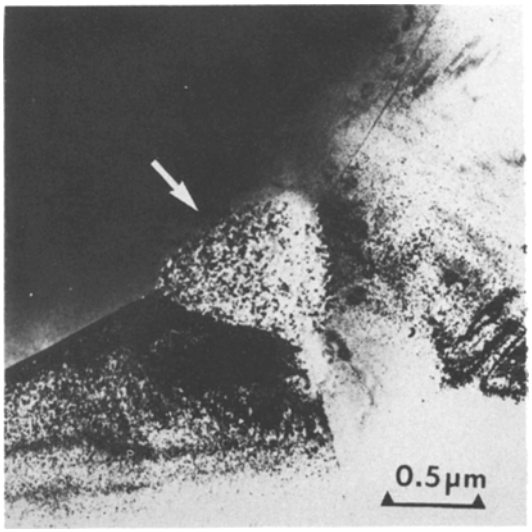

Figure 3 A bright-field image of small particles at grain boundary triple-point (arrowed).

In specimens which underwent more extensive current-blackening, the transformation was more extensive, and sometimes an entire grain had transformed to the dark polycrystalline aggregates (Fig. 5). Individual crystallites in such samples appear more well-defined and larger. The diffraction pattern again shows primitive-cubic reflections along with the fluorite-phase reflections.

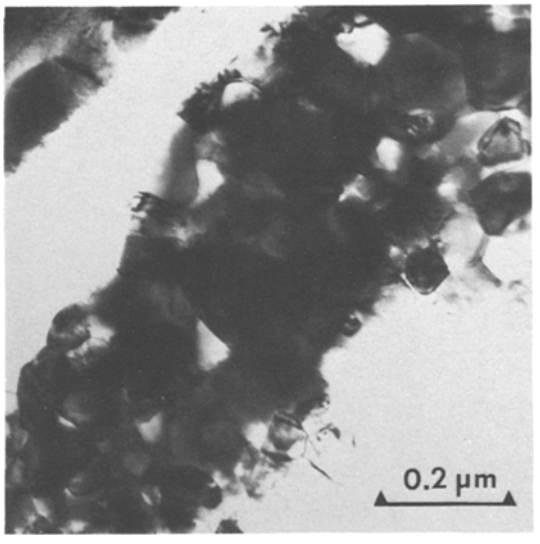

Figure 5 A bright-field image of SSZ which underwent more extensive current-blackening. The grain sizes are much larger than the ones observed in Figs. 2 and 3.

4. Summary and conclusions

Based on the TEM observations, it is postulated that heavy-current treatment results in nucleation of polycrystalline aggregates along the grain boundaries and at defects within the lattice (inclusions and second-phase particles), which then grow at the expense of the matrix phase as blackening proceeds. These polycrystalline aggregates are probably the same phase which was observed in previous SEM, X-ray and optical studies [8, 10, 15]. The polycrystalline phase has the lattice parameter closely matching those of the parent cubic-fluorite phase. The presence of weak reflections corresponding to that of a primitive-cubic structure suggests, however, that the grain boundary phase may consist in part of non-stoichiometric zirconium suboxides (ZrO_{2-x}), which has lost a sufficient amount of oxygen from the lattice to lose the translational symmetry of the fluorite structure. Direct determination of oxygen deficiency postulated for this phase is not possible, however, by any present TEM analysis technique. The size of individual crystallites in the aggregate correspond reasonably well with the size of "colloidal particles" suggested by Wright *et al.* [3]. The fact that no change in elastic constant and lattice parameter are observed upon blackening in previous studies [2, 17] agrees with our observation that the polycrystalline phase retains, for the most part, the structure of the parent phase.

The development of the suboxide upon current-blackening is consistent with observed property changes. Similar to the behaviour in some other oxide systems that have been more extensively studied, such as Nb_2O_5, V_2O_5 and TiO_2, the formation of the suboxide is accompanied by changes in colour and conductivity arising from new electronic states [18]. The development of dark polycrystallites selectively at the grain boundaries and their later coarsening is also consistent with the degradation in mechanical properties.

Acknowledgement

The authors wish to express their appreciation to the Department of Energy, Washington, DC under contract EY-76-03-0326 PA No. 37. One of the authors (TY) thanks IBM Student Fellowship for support.

References

1. M. KLIETZ, PhD thesis, University of Grenoble (1968).
2. R. E. W. CASSELTON, J. S. THORP and D. A. WRIGHT, *Proc. Brit. Ceram. Soc.* **19** (1970) 265.
3. D. A. WRIGHT, J. S. THORP, A. AYPAR and H. P. BUCKLEY, *J. Mater. Sci.* 8 (1973) 876.
4. J. S. THORP, A. AYPAR and J. S. ROSS, *ibid.* 7 (1972) 729.
5. H. YANAGIDA, R. J. BROOK and F. A. KROGER, *J. Electrochem. Soc.* **117** (1970) 593.
6. M. GUILLOU, J. MILLET and S. PALOUS, *Electrochim. Acta* **13** (1968) 1411.
7. R. E. W. CASSELTON, *J. Appl. Electrochem.* 4 (1974) 25.
8. R. E. W. CASSELTON, in "Electromotive Force Measurements in High Temperature Systems", edited by C. B. Alcock, (Elsevier, New York, 1968) pp. 151–7.
9. S. PIZZINI, M. BIANCHI, A. CORRADI and C. MARI, *ibid.* 4 (1974) 7.
10. T. GUR, PhD thesis, Standford University (1976).
11. N. M. PODASCHEWSKY, *Phys. Zeit. Sowjetunion* 8 (1953) 81.
12. D. R. FRANKL and T. A. READ, *Phys. Rev.* 89 (1953) 663.
13. E. AERTS, S. AMELINCKX and W. DEKEYSER, *Acta Metall.* 7 (1959) 29.
14. F. M. SPIRIDONOV, L. N. POPOVA and R. Ya. POPILSKII, *J. Solid State Chem.* 2 (1970) 430.
15. R. RUH, H. J. GARROTT, R. F. DOMAGALA and V. A. PATEL, *J. Amer. Ceram. Soc.* **60** (1977) 399.
16. F. K. MOGHADAM, T. YAMASHITA and D. A. STEVENSON, "Advances in Ceramics" Vol. 3, edited by A. H. Heuer and L. W. Hobbs (1981) p. 364.
17. J. M. FARLEY, J. S. THORP, J. S. ROSS and G. A. SAUNDERS, *J. Mater. Sci.* 7 (1972) 475.
18. L. EYRING and M. O'KEEFFE (eds), Proceedings of the Institute of Advanced Study of the Chemistry of Extended Defects Non-Metallic Solids (North Holland, 1970).

Received 10 May
and accepted 19 November 1982